Aptamer Functionalized Hydrogel Microparticles for Fast Visual Detection of Mercury(II) and Adenosine

Youssef Helwa[†], Neeshma Dave[†], Romain Froidevaux, Azadeh Samadi, and Juewen Liu*

Department of Chemistry, Waterloo Institute for Nanotechnology, University Of Waterloo

Waterloo, Ontario, N2L 3G1, Canada

Email: liujw@uwaterloo.ca

[†] These authors contributed equally to the work.

Abstract

With a low optical background, high loading capacity, and good biocompatibility, hydrogels are ideal materials for immobilization of biopolymers to develop optical biosensors. We recently immobilized mercury and lead binding DNAs within a monolithic gel and demonstrated ultra-sensitive visual detection of these heavy metals. The high sensitivity was attributed to the enrichment of the analytes into the gels. The signaling kinetics was slow, however, taking about one hour to obtain a stable optical signal due to a long diffusion distance. In this work we aim to understand the analyte enrichment process and improve the signaling kinetics by preparing hydrogel microparticles. DNA-functionalized gel beads were synthesized using an emulsion polymerization technique and most of the beads were between 10 and 50 µm. Acrydite-modified DNA was incorporated by co-polymerization. Visual detection of 10 nM Hg^{2+} was still achieved and a stable signal was obtained in just two minutes. The gel beads could be spotted to form a microarray and dried for storage. A new visual sensor for adenosine was designed and immobilized within the gel beads. The adenosine aptamer binds its target about 1000-fold less tightly compared to the mercury binding DNA, allowing a comparison to be made on analyte enrichment by aptamer-functionalized hydrogels.

Keywords: aptamers, hydrogels, microparticles, fluorescence, mercury, adenosine

Introduction

Biosensors rely on biomolecules for target recognition.[1] While high specificity and strong binding affinity can often be achieved, biomolecules such as nucleic acids and proteins are susceptible to denaturation and degradation. To effectively protect these molecules and interface them with devices at the same time, much research effort has been devoted to developing materials for biosensor

immobilization, including on gold,[2,3] silica,[4] carbon nanotubes,[5,6] graphene oxide,[7,8] lipid bilayers,[9]

paper materials,[10] and hydrogels.[11,12] Hydrogels are particularly attractive for making optical sensors.[13-19]

Biomolecular immobilization occurs not only on gel surface but also throughout the whole gel matrix, allowing for high loading capacity. Due to its porous nature, all the immobilized probes are accessible to generate a strong signal. In addition, since the majority of hydrogel volume is water, attached biomolecules can easily maintain their function.[20] These properties also enable hydrogels to be used for controlled protein release and for designing artificial tissues.[21-25] Since most hydrogels are transparent, optical sensors do not suffer from background color or fluorescence. Hydrogels can be made into various forms including nano- and microparticles, thin films and monoliths.[26] Monolithic gels are easy to prepare, but molecular diffusion within the gel may take a long time. We recently reported DNAfunctionalized monolithic hydrogels for Hg^{2+} and Pb^{2+} detection and more than 1 hour was required to

reach a stable signal.[16,17,27] Therefore, one goal of the current work is to improve the signaling kinetics. These gels also possess unique volume-dependent sensitivity. In biosensor research, detection limit is typically governed by analyte concentration. These gels, however, are able to absorb analytes so that the analyte concentration inside the gel is much higher than that in the surrounding buffer. For both Hg^{2+} and Pb^{2+} detecting gels, visual detection of low nM metal ions was achieved if the sample volume was 50 mL. Thus it is interesting to test whether the analyte enrichment can also be achieved for other aptamers with a lower binding affinity.

In this work, we aim to achieve two goals. First, we report a convenient route to synthesize hydrogel microparticles with covalently attached DNA probes. Compared to monolithic gels of the same formulation, the rate of mercury signaling was improved by ~20-fold for the gel beads. Second, we designed a new visual sensor for adenosine detection. The adenosine aptamer has a dissociation constant (K_d) of ~6 µM, which is much weaker than the low nM affinity for the two metal binding DNAs. As a result, immobilization in gel did not improve sensitivity for adenosine detection, highlighting the importance of aptamer affinity for target enrichment.

Experimental Section

Chemicals. All DNA samples were purchased from Integrated DNA Technologies (Coralville, IA) and purified by standard desalting. Acrylamide and bis-acrylamide, Span 80, mercury perchloride, copper sulfate, zinc chloride, manganese chloride, cobalt chloride, lead acetate, magnesium chloride, calcium chloride, and thiazole orange (TO) were obtained from Sigma-Aldrich (St. Louis, MO). Ammonium persulphate (APS) and N,N,N',N'-tetramethylethylenediamine (TEMED) were purchased from VWR (Mississauga, ON) Sodium nitrate, adenosine, cytidine, uridine, guanosine, ethidium bromide, and 4(2-hydroxyethyl)-1-piperazineethanesulfonic acid (HEPES) were purchased from Mandel Scientific (Guelph, ON). 10,000× SYBR Green I (SG) in dimethyl sulfoxide (DMSO), PicoGreen, and SYTO-13 were purchased from Invitrogen (Carlsbad, CA).

Hydrogel microparticle preparation. Polyacrylamide hydrogel microparticles were prepared using emulsion polymerization.[28] The aqueous phase (2 mL total) contained 4 µL APS, acrylamide (0.18 g) and bis-acrylamide (0.02 g) and a final of 2 µM Acrydite-modified DNA. The oil phase consisted of cyclohexane (2 mL) and 100 µL Span 80 as the surfactant. The aqueous phase was dispersed into the oil phase in a 10 mL glass vial. The solution was stirred at 800 rpm for 5 min in an ice bath to form an inverse suspension. After purging the emulsion with nitrogen gas for 2 min, the polymerization was

initiated by adding TEMED (4 µL). The polymerization was continued for 4 hr under the 800 rpm stirring at room temperature. Afterwards, the stirring was stopped and the emulsion phase separated to allow the removal of the top cyclohexane layer. Each 100 µL of the aqueous phase was dissolved in 1 mL ethanol. After 1 hr soaking in ethanol, the solution was centrifuged for 15 min at 15000 rpm and the ethanol was removed. The gel beads were soaked in 1 mL of water for 30 min and washed by centrifugation. This washing process was repeated 4 times in water to remove unreacted monomers and initiators. Finally, the gels were dispersed at a concentration of 10 mg/mL (considering only the dry mass of the gel). The size distribution of the hydrogel beads were obtained by measuring ~200 particles under an optical microscope.

Hg^{2+} detection. For visual detection, 200 µL of gel beads were added to each tube containing 1.2 mL of buffer A (20 mM $NaNO_3$, 10 mM HEPES, pH 7.6) with various amounts of Hg^{2+} and 100 nM SG. The samples were incubated for 20 min and 1 mL of supernatant was removed. To this 250 nM of SG was added and the samples were observed using a blue light transilluminator (Invitrogen Safe Imager 2.0, excitation wavelength = 470 nm) and the fluorescence was recorded using a digital camera (Canon PowerShot SD1200 IS). To observe under a fluorescence microscope, 2 µL of the beads were spotted onto a glass slide and imaged using the cube for FAM fluorophore. The exposure time and other imaging conditions were set to be the same for all the samples. Fluorescence intensity was quantified using Adobe Photoshop.

Kinetics. The kinetic experiment was carried out using a fluorometer (Eclipse, Varian) by exciting at 480 nm, and the emission at 520 nm was monitored. Free DNA (20 nM) was dissolved in 600 µL buffer A and its background fluorescence was monitored for ~2 min before 100 nM SG was added. After another 5 min, 1 µM Hg^{2+} was added. For the gel microparticles, 20 µL of 10 mg/mL gel beads were dispersed

in 600 µL of the same buffer and the same amount of SG and Hg^{2+} was added. The cuvette was agitated before each measurement to ensure that the beads were homogeneously dispersed in buffer.

Drying and rehydration. A glass microscope cover slide was briefly washed with water and dried with ethanol. To dry the beads, 2 µL of 40 mg/mL gel beads dispersed in water were spotted using a micro-pipette onto the slide. The beads were dried overnight at room temperature. Rehydration was performed using 4 µL of 5 µM SG in the presence or absence of 2 µM Hg^{2+} in buffer A. The signal was observed using the transilluminator and recorded with a digital camera.

Adenosine detection. In each tube 1 mL of 25 mM HEPES and 50 µL of 10 mg/mL hydrogel beads were added. The sample was added to a water bath at 80 °C and allowed to cool to room temperature. After which adenosine was added and the sample was then centrifuged and 900 µL of the supernatant was removed. To the pellet, 1 µM of SYTO-13 was added. The gels were imaged using the transilluminator. For dye screening using the free DNA, 0.5 µM of the adenosine aptamer was dissolved in buffer (5 mM $NaNO_3$ 8 mM Tris nitrate, final volume = 100 µL). The sample was heated to 80 °C and cooled to 25 °C before adenosine (2 mM) and the dyes (2.5 µM) were added.

Results and Discussion

DNA-functionalized hydrogel microparticles. Mercury is a highly toxic heavy metal and its detection has attracted a lot of research efforts.[29] A recent development is the use of thymine-rich DNA for Hg^{2+} binding.[30] In this work, we immobilized a Hg^{2+} binding DNA (Figure 1A) into a hydrogel microparticle to achieve fast visual detection (Figure 1B). Hydrogel microparticles can be prepared by using either emulsion templated polymerization or lithographic techniques.[28,31-33] We chose the former method to achieve a high yield. In a typical synthesis, Acrydite-modified Hg^{2+}-binding DNA, acrylamide, and bisacrylamide were mixed. A water-in-oil emulsion was formed using Span 80 as the surfactant and

cyclohexane as the oil phase. After polymerization, the gel particles were washed and dispersed in water. We were able to obtain grams of gel beads in each synthesis.
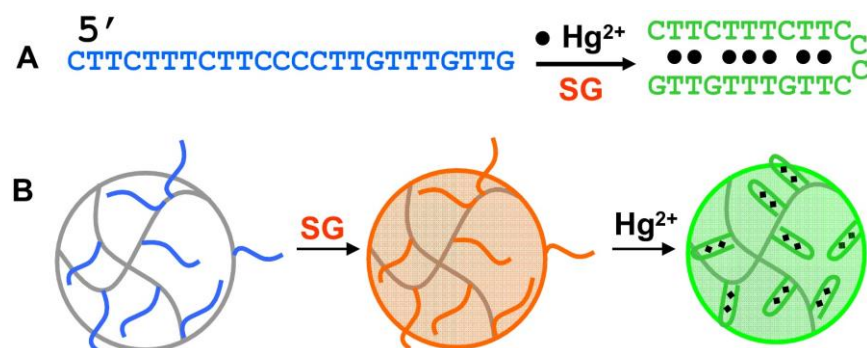

Figure 1. (A) The sequence of the Hg^{2+} binding DNA and its reaction with Hg^{2+} and SG. The 5′-end of this DNA was modified with an Acrydite group for hydrogel attachment. (B) Covalent DNA immobilization within a polyacrylamide hydrogel and interaction with Hg^{2+} and SG produced a visual fluorescence signal.

The gel beads were spherical under an optical microscope (Figure 2A), with most being in the size range from 10 to 50 μm (Figure 2C, black bars). By calculating the mass percentage, an average size around 30 μm was observed (red bars). These beads were large enough to be easily precipitated in water. After staining the DNA using SYBR Green I (SG), a fluorescence signal was obtained using blue light excitation (Figure 2B), and the fluorescent particles co-localized with the image obtained using the transmission mode, suggesting the DNA was inside the gel. As a control, if no acrydite-DNA was added during gel preparation, no fluorescence was observed from the beads even after the addition of SG (Figure S1, Supporting Information), confirming that the DNA-functionalized gel beads were successfully prepared.
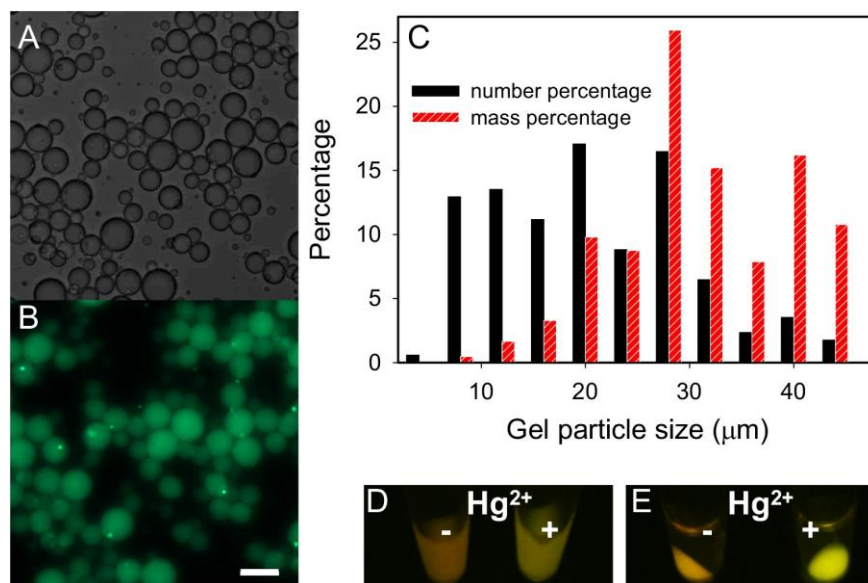
Figure 2. Hydrogel microparticle characterization using optical microscopy under transmission light (A) and fluorescence mode (B). Scale bar = 40 μm. (C) Size distribution of the gel beads. Fluorescence of the gel beads in the absence or presence of 10 μM Hg^{2+} when the beads were uniformly dispersed in buffer (D) or after centrifugation (E). Buffer A (20 mM $NaNO_3$, 10 mM HEPES, pH 7.6) was used for mercury detection.

Visual Hg^{2+} detection. The Hg^{2+} binding DNA in Figure 1A has been widely used for Hg^{2+} recognition. This particular DNA contains seven hypothetical Hg^{2+} binding sites. A long DNA with many Hg^{2+} binding sites can produce a larger conformational change and thus good signal-tobackground ratio. In the absence of Hg^{2+}, this DNA is a random coil and binds to SG weakly producing yellow fluorescence.[17] In the presence of Hg^{2+}, the DNA forms a hairpin, upon which SG can bind strongly to give intense green fluorescence. As shown in Figure 2D, this expected result was obtained after incubating the gel beads with 5 μM SG with or without 10 μM Hg^{2+} under the excitation of 470 nm light. To confirm that the

fluorescence was emitted from the gel instead of free DNA in solution, the two tubes were centrifuged and imaged again (Figure 2E); the fluorescent beads were pelletized at the bottom and the supernatant solution was non-fluorescent. This result confirmed that the gel beads were capable of visual detection.
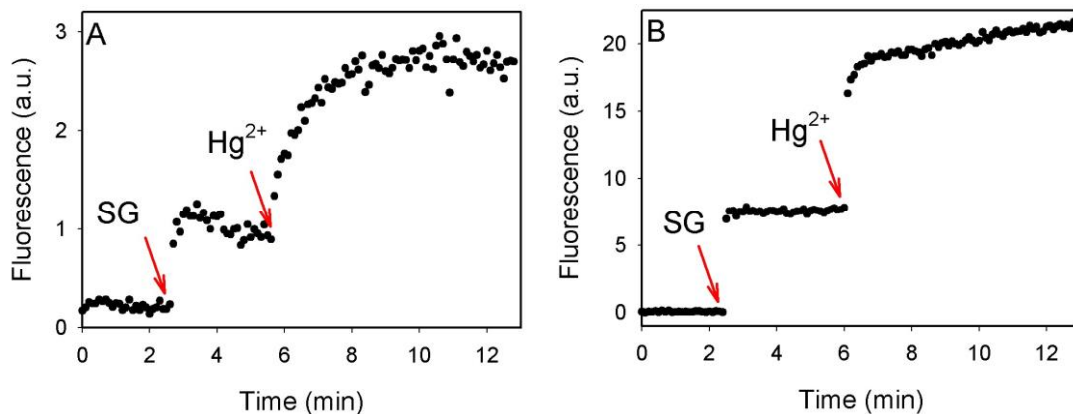

Figure 3. Fluorescence signaling kinetics of DNA-functionalized hydrogel microparticles (A) or free DNA (B). The arrows indicated the time points when SG (100 nM) and Hg^{2+} (1 µM) were respectively added.

Kinetics of signal change. One of the main motivations to develop hydrogel microparticles was to achieve a short diffusion distance and thus reach a stable signal faster. The thickness of the previously reported monolithic gels was ~2 mm while the average size of the gel particles was only ~30 µm. Given a size difference of >50-fold, the diffusion time is expected to reduce significantly. To measure signaling kinetics, hydrogel microparticles were dispersed in a cuvette. As shown in Figure 3A, a fast increase in the fluorescence signal was observed after addition of SG. The signal was stabilized in about half a minute. Addition of 1 µM Hg^{2+} resulted in a further fluorescence increase, which was stabilized in ~3 min (rate of signal increase = 1.0 min^{-1}). For comparison, the free DNA was also tested under the same conditions and it reached equilibrium even more quickly for both additions (Figure 3B). Compared to the ~1 hr needed for the monolithic gels,[17] the improvement on the signaling kinetics was at least 20-fold.
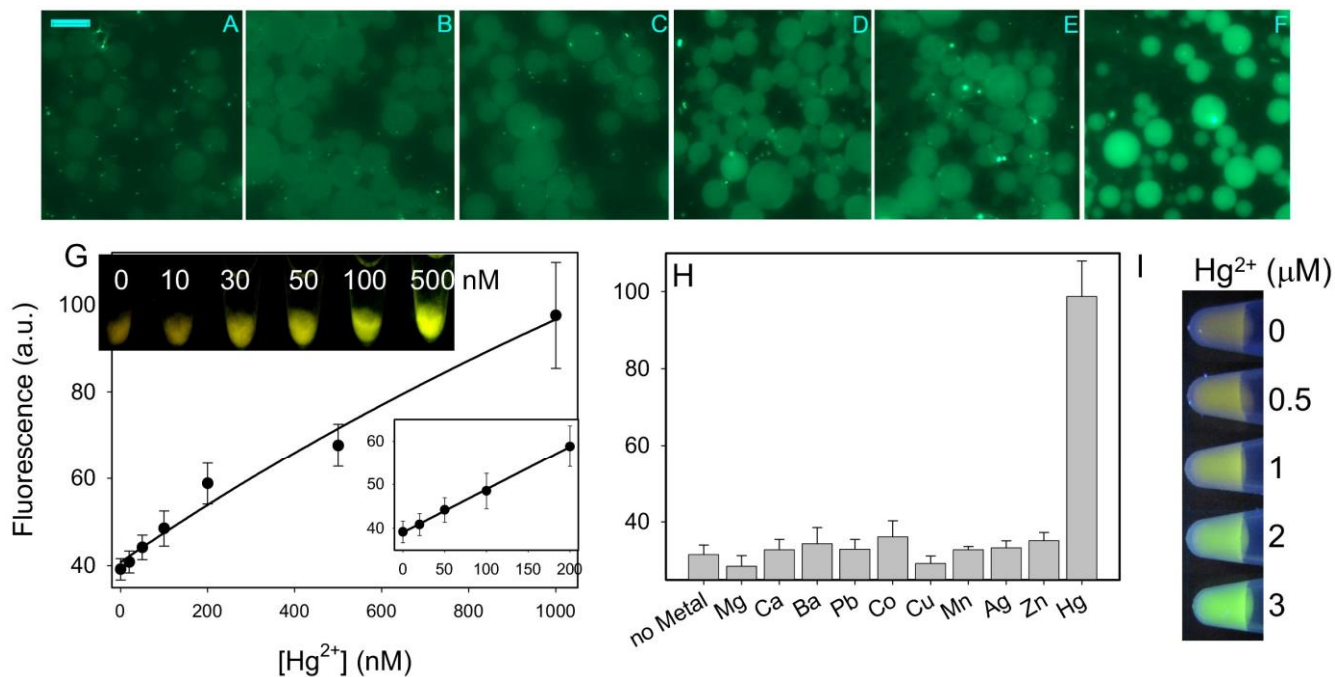
Figure 4. Fluorescence micrographs of the gel beads exposed to varying concentrations of Hg^{2+}. (A) 0; (B) 50 nM; (C) 100 nM; (D) 200 nM; (E) 500 nM (F) 1 μM. Scale bar = 40 μm. (G) Quantification of signal intensity from the microscope micrographs. The lower concentration region is shown in the bottom inset. Inset on the upper corner: a digital camera picture of gel beads exposed to various concentrations of Hg^{2+}. (H) Selectivity test with 10 μM competing metals and the mercury concentration was 1 μM. (I) Visual detection of Hg^{2+} using the non-immobilized sensor.

Mercury detection. To characterize the sensor performance, we mixed the gel beads with various concentrations of Hg^{2+} and observed them using a fluorescence microscope (Figures 4A-F). The fluorescence intensity was significantly increased in the presence of Hg^{2+}. The signal was quantified and plotted in Figure 4G and its lower inset shows the response in the low concentration region. By visual inspection of the gel beads, even 10 nM Hg^{2+} can be visually detected (the upper inset of Figure

9

4G) and 30 nM Hg^{2+} produced a much better distinction. Since the human eye cannot detect 10-30 nM

SG fluorescence, this sensitive visual detection suggested Hg^{2+} enrichment within the gel. For example,

visual detection of Hg^{2+} using non-immobilized DNA was achieved only in the presence of higher than

500 nM Hg^{2+} (Figure 4I). To test the reproducibility of synthesis, we prepared a total of three batches of

DNA-functionalized gel beads, and similar sensitivity was observed for each batch. Therefore, although

the size distribution of the gels was relatively large, the performance was not affected. To test specificity,

the gel beads were incubated with 10 μM of various metal ions, of which only Hg^{2+} showed significant

fluorescence enhancement (Figure 4H). Although Ag^+ also produced some fluorescence increase, this

fluorescence was quickly bleached during imaging and did not show up for quantification. Therefore, the

high selectivity was maintained after gel immobilization. We have further performed detection in Lake

Ontario water and a similar visual detection limit of ~30-50 nM Hg^{2+} was achieved (Figure S2,

Supporting Information).

An important feature of hydrogel microparticles is that they can be processed easily. After

dispersed in an aqueous solution, the gel beads can be applied on a solid substrate. The gel matrix helps

to retain DNA on the substrate. To test this, we casted a small array using a micro-pipettor to dispense 2

μL gel beads onto a glass slide. After overnight drying, a thick film was formed with the diameter of each

spot being ~4 mm (Figure 5A). The dried beads were then rehydrated using either 5 μM SG or the same

buffer containing also 2 μM Hg^{2+} (Figure 5B). The spots without Hg^{2+} showed an orange fluorescence

while the spots with Hg^{2+} were yellowish green, although the fluorescence intensities of these samples

were quite similar. For comparison, freshly prepared gel beads were also spotted; the samples with Hg^{2+}

showed stronger green fluorescence than the samples without Hg^{2+} (Figure 5C). To understand the effect

of drying, a micrograph of the gel beads after rehydration is shown in Figure 5D. The spherical shape of

the beads was observed, indicating that the overall structure of the beads was not damaged by drying. The smeared features on this micrograph were due to the out-of-focus beads.

Therefore, the increased background fluorescence after drying (Figure 5B) is attributed to changes in gel internal structures, which might be relieved by adding preserving agents such as sucrose or trehalose.
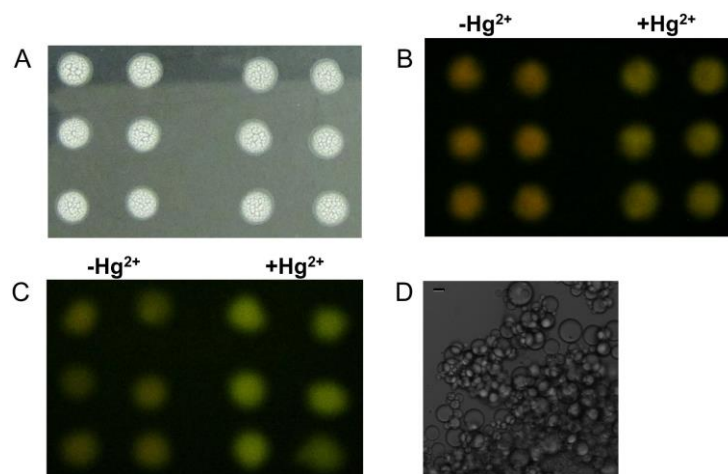

Figure 5. (A) A photograph of a dried array of hydrogel microparticles. The diameter of each spot was ~ 4 mm. Fluorescence micrograph of the dried gels after rehydration (B) or freshly prepared gels (C) in the presence (the six spots on the right) or absence (on the left) of 2 μM Hg^{2+}. (D) A micrograph of the rehydrated gel beads. Scale bar = 20 μm.

Visual detection of adenosine. For visual detection, the human eye needs ~1 μM fluorophore. If each target molecule can only light up one fluorophore, visual inspection can only detect ~1 μM analyte. One way to increase sensitivity is to make each analyte turn over the production of more than one fluorophore, which has been demonstrated in many signal amplification systems.[34] We took a different route to rely on the specific and strong binding between DNA aptamers and target analytes to enrich analytes into hydrogels. The fact that even 10 nM Hg^{2+} can be visually detected indicates the enrichment of Hg^{2+} in the gel beads. Since the DNA concentration in the gel beads was ~2 μM, a maximal of 14 ☐M Hg^{2+} could be bound by the DNA. Both Hg^{2+} and Pb^{2+} binding DNAs have low nM affinities for their respective

11

target. To test generality, we aim to immobilize an aptamer with a weaker binding affinity. The adenosine aptamer was chosen for this purpose since it is a well-studied model aptamer (K_d = ~6 μM).[35]
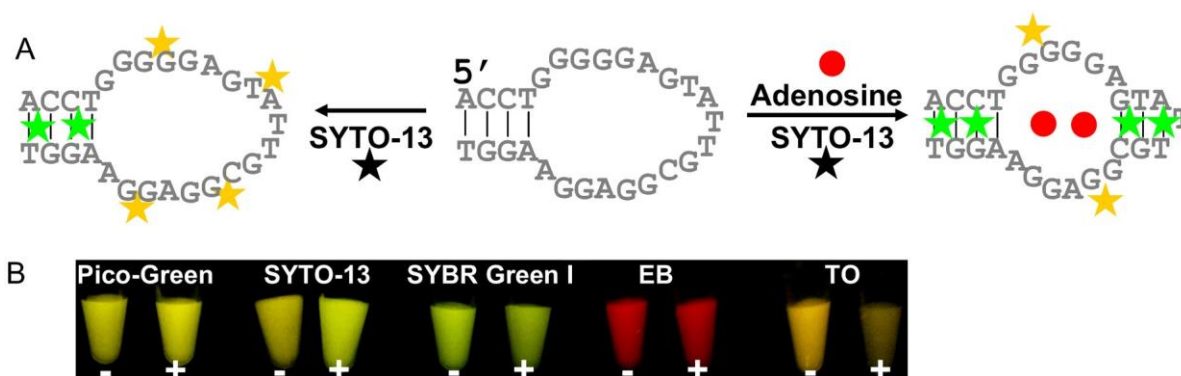

Figure 6. (A) Schematics of visual detection of adenosine using an adenosine binding aptamer and SYTO-13. (B) Screening for DNA binding dyes for visual detection of adenosine.

An appropriate fluorescent sensor for adenosine needs to be identified for immobilization. A preferred sensor should contain just a single DNA strand, can be modified on its 5′-end with an Acrydite group, produce a visual response, and be cost-effective. By studying the literature, although a large number of adenosine sensors have been reported, none could satisfy all the requirements.[36] Labelfree detection is a more desirable approach, but no sensor suitable for visual detection in hydrogel was identified. Therefore, we need to design a new visual sensor for adenosine detection.[37]

The visual sensors for Hg^{2+} and Pb^{2+} used for immobilization were based on DNA binding dyes. SG, a duplex binding dye, was used for Hg^{2+} detection and thiazole orange (TO, a quadruplex binding dye) was used for Pb^{2+}.[17,27] These dyes show a yellow fluorescence upon binding to the free DNAs. In the presence of the target metal ions, the emission shifts to green. Along this line, we aim to test whether this method can be used for detecting adenosine. The aptamer sequence is shown in Figure 6A.

We tested five DNA binding dyes and only SYTO-13 showed a yellow-to-green fluorescence change along with an overall increased quantum yield (Figure 6B), while other dyes did not produce response favorable for visual detection. Since the structure of SYTO-13 has not been disclosed, it is difficult to speculate the exact signaling mechanism. SG can significantly increases duplex DNA melting temperature, but it is not the case for SYTO-13, which indicates a major difference in their interaction with DNA and might contribute to SYTO-13's signaling ability for the adenosine aptamer.[38]
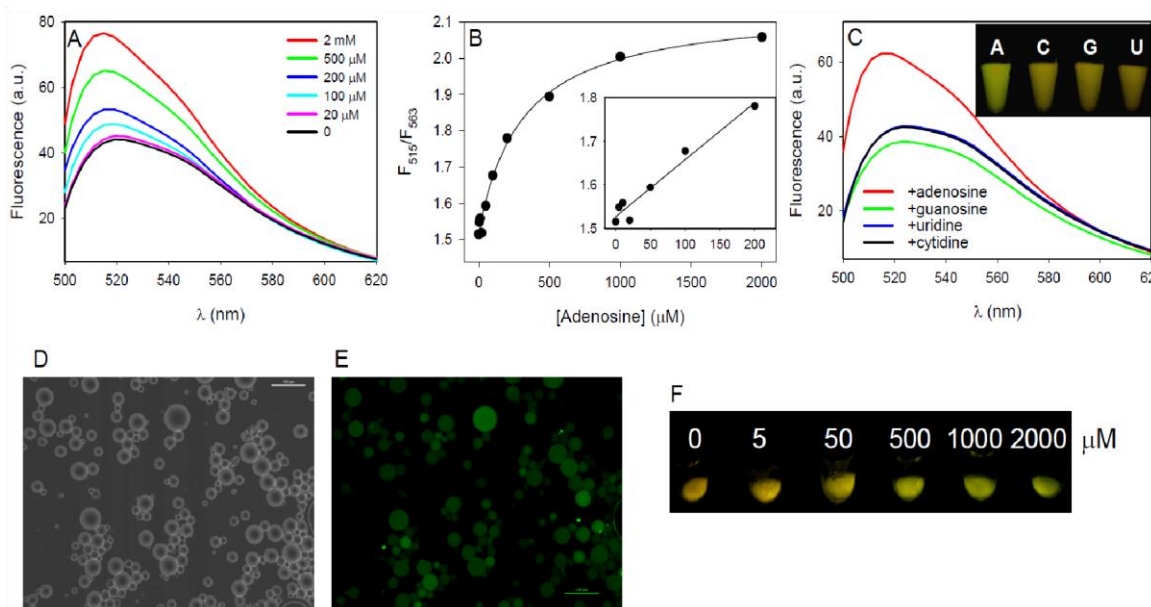

Figure 7. (A) Fluorescence spectra of the adenosine DNA aptamer with SYTO-13 in the presence of various concentrations of adenosine. (B) Ratiometric plot of the sensor signal as a function of adenosine concentration. (C) Selectivity test. Inset shows the visual fluorescence in the presence of 2 mM various ribonucleotides. Optical micrographs of hydrogel beads with the adenosine aptamer in the transmission mode (D) and fluorescence mode (E). (F) Visual response of adenosine detection by the gel beads.

Since SYTO-13 provided the best visual response, we mixed the aptamer and SYTO-13 with various concentrations of adenosine and their fluorescence spectra were collected (Figure 7A). In the absence of adenosine, a broad bump was observed. Addition of adenosine resulted in an increase of the

13

515 nm peak. Therefore, the ratio of fluorescence intensity at 515 nm over 563 nm was used for quantification. The former wavelength was assigned to SYTO-13 binding to duplex DNA and the latter to binding to ss-DNA. The titration curve is shown in Figure 7B and the detection limit was determined to be 45 μM. In terms of selectivity, all of the other ribo-nucleosides including guanosine, cytidine, and uridine showed a yellowish fluorescence and only adenosine gave a more intense green fluorescence (Figure 7C).

Next adenosine aptamer functionalized hydrogel microparticles were prepared using the same protocol as for the Hg^{2+} gels. The gel beads showed a similar size distribution (Figure 7D) and were fluorescent after staining with SYTO-13 (Figure 7E). Their visual response as a function of adenosine concentration was recorded (Figure 7F); ~50 μM adenosine was required to produce a visual color change and a significant change was observed only with 500 μM adenosine. This sensitivity was similar to that for the non-immobilized sensor (Figure 7B). Therefore, immobilization did not improve the visual sensor performance in this case. The relatively small fluorescence signal change in the adenosine sensor may also contribute to its limited sensitivity.

This study suggests the importance of binding affinity for target analyte enrichment in immobilized sensors. The K_d of the Hg^{2+} and Pb^{2+} aptamers are in the low nM region and close to quantitative binding can be achieved. Therefore, immobilizing μM DNA probe inside gel could eventually accumulate μM metal ions to produce signal necessary for visual detection. In other words, these metal sensors are limited by the detector (i.e. the human eye). For the adenosine aptamer, however, quantitative binding cannot be realized due to weak binding affinity. To push a large fraction of immobilized aptamer to bind, the adenosine concentration needs to be much greater than its K_d, which is already in the high μM region for this sensor (Figure 7B) and is higher than the DNA concentration within the gel (e.g. 2 μM). In other words, the adenosine concentration in the gel is already higher than

the DNA concentration in gel and the aptamer can produce only a negligible enrichment effect. Therefore, to achieve low nM sensitivity for visual detection in hydrogel, the aptamer affinity needs to be high.

Conclusions

In summary, we reported the preparation of DNA-functionalized hydrogel microparticles for visual detection of both Hg^{2+} and adenosine. Compared to monolithic gels, microparticles showed much faster kinetics of signal generation. At the same time, they can still be easily handled. For example, with a simple centrifugation step, the gel beads can be washed and precipitated. Detection can be achieved via the naked eye or by microscope at the individual particle level. Since the DNA was immobilized not only on the gel surface but also inside the gel matrix, a high loading capacity was achieved to generate strong visual signals. Finally, since the particles can be easily dispersed in water, they can be processed by casting onto a solid substrate for drying and rehydration can be easily achieved by simply adding buffer. Therefore, such hydrogels are useful soft materials for analytical applications. By comparing aptamers with ~1000-fold difference in K_d, the mechanism for ultrahigh sensitivity in visual metal detection was confirmed.

Supporting Information Available: Control gels without DNA and detection in lake water. This material is available free of charge via the Internet at http://www.acs.org.

References:

(1)   (a) Willner, I.; Zayats, M. *Angew. Chem., Int. Ed.* **2007**, *46*, 6408-6418. (b) Wang, H.; Yang, R. H.; Yang, L.; Tan, W. H. *Acs Nano* **2009**, *3*, 2451-2460. (c) Rosi, N. L.; Mirkin, C. A. *Chem. Rev.* **2005**, *105*, 1547-1562. (d) Liu, J.; Cao, Z.; Lu, Y. *Chem. Rev.* **2009**, *109*, 1948–1998. (e) Zhou, M.; Dong, S. *Acc. Chem. Res.* **2011**, *44*, 1232-1243. (f) Li, D.; Song, S. P.; Fan, C. H. *Acc. Chem. Res.* **2010**, *43*, 631-641.

(2)   Elghanian, R.; Storhoff, J. J.; Mucic, R. C.; Letsinger, R. L.; Mirkin, C. A. *Science* **1997**, *277*, 1078-1080.

(3)   Zhao, W.; Brook, M. A.; Li, Y. *Chembiochem* **2008**, *9*, 2363-2371.

(4)   Avnir, D.; Coradin, T.; Lev, O.; Livage, J. *J. Mater. Chem.* **2006**, *16*, 1013-1030.

(5)   Yang, R. H.; Jin, J. Y.; Chen, Y.; Shao, N.; Kang, H. Z.; Xiao, Z.; Tang, Z. W.; Wu, Y. R.; Zhu, Z.; Tan, W. H. *J. Am. Chem. Soc.* **2008**, *130*, 8351-8358.

(6)   Zhu, Z.; Yang, R.; You, M.; Zhang, X.; Wu, Y.; Tan, W. *Anal. Bioanal. Chem.* **2010**, *396*, 73-83.

(7)   Lu, C. H.; Yang, H. H.; Zhu, C. L.; Chen, X.; Chen, G. N. *Angew. Chem. Int. Ed.* **2009**, *48*, 4785-4787.

(8)   Loh, K. P.; Bao, Q.; Eda, G.; Chhowalla, M. *Nat Chem* **2010**, *2*, 1015-1024.

(9)   Sackmann, E.; Tanaka, M. *Trends Biotechnol.* **2000**, *18*, 58-64.

(10)   Ali, M. M.; Aguirre, S. D.; Xu, Y. Q.; Filipe, C. D. M.; Pelton, R.; Li, Y. F. *Chem. Comm.* **2009**, 6640-6642.

(11)   Liu, J. *Soft Matter* **2011**, *7*, 6757-6767.

(12)   Nayak, S.; Lyon, L. A. *Angew. Chem. Int. Ed.* **2005**, *44*, 7686-7708.

(13)   Yang, H. H.; Liu, H. P.; Kang, H. Z.; Tan, W. H. *J. Am. Chem. Soc.* **2008**, *130*, 6320-6321.

(14)   Zhu, Z.; Wu, C. C.; Liu, H. P.; Zou, Y.; Zhang, X. L.; Kang, H. Z.; Yang, C. J.; Tan, W. H. *Angew. Chem. Int. Ed.* **2010**, *49*, 1052-1056.

(15)   Cheng, E. J.; Xing, Y. Z.; Chen, P.; Yang, Y.; Sun, Y. W.; Zhou, D. J.; Xu, L. J.; Fan, Q. H.; Liu, D. S. *Angew. Chem. Int. Ed.* **2009**, *48*, 7660-7663.

(16)   Joseph, K. A.; Dave, N.; Liu, J. *ACS Appl. Mater. Inter.* **2011**, *3*, 733–739.

(17)   Dave, N.; Huang, P.-J. J.; Chan, M. Y.; Smith, B. D.; Liu, J. *J. Am. Chem. Soc.* **2010**, *132*, 12668–12673.

(18)   Baeissa, A.; Dave, N.; Smith, B. D.; Liu, J. *ACS Appl. Mater. Inter.* **2010**, *2*, 3594-3600.

(19)   El-Hamed, F.; Dave, N.; Liu, J. *Nanotechnology* **2011**, *22*, 494011.

(20)   Peppas, N. A.; Hilt, J. Z.; Khademhosseini, A.; Langer, R. *Adv. Mater.* **2006**, *18*, 1345-1360.

(21)   Soontornworajit, B.; Zhou, J.; Wang, Y. *Soft Matter* **2010**, *6*, 4255-4261.

(22)   Soontornworajit, B.; Zhou, J.; Shaw, M. T.; Fan, T. H.; Wang, Y. *Chem. Comm.* **2010**, *46*, 1857-1859.

(23)   He, X.; Wei, B.; Mi, Y. *Chem. Comm.* **2010**, *46*, 6308-6310.

(24)   Soontornworajit, B.; Zhou, J.; Snipes, M. P.; Battig, M. R.; Wang, Y. *Biomaterials* **2011**, *32*, 6839-6849.

(25)   Xing, Y. Z.; Cheng, E. J.; Yang, Y.; Chen, P.; Zhang, T.; Sun, Y. W.; Yang, Z. Q.; Liu, D. S. *Adv. Mater.* **2011**, *23*, 1117-1121.

(26)   Tokarev, I.; Minko, S. *Soft Matter* **2009**, *5*, 511-524.

(27)   Jacobi, Z. E.; Li, L.; Liu, J. *Analyst* **2012**, *137*.

(28)   Liu, X. D.; Murayama, Y.; Matsunaga, M.; Nomizu, M.; Nishi, N. *Int. J. Biol. Macromol.* **2005**, *35*, 193-199.

(29)   Nolan, E. M.; Lippard, S. J. *Chem. Rev.* **2008**, *108*, 3443-3480.

(30)   (a) Ono, A.; Togashi, H. *Angew. Chem., Int. Ed.* **2004**, *43*, 4300-4302. (b) Wang, J.; Liu, B. *Chem. Comm.* **2008**, 4759-4761. (c) Wang, Z.; Lee, J. H.; Lu, Y. *Chem. Comm.* **2008**, 60056007. (d) Chiang, C. K.; Huang, C. C.; Liu, C. W.; Chang, H. T. *Anal. Chem.* **2008**, *80*, 37163721. (e) Lee, J.-S.; Han, M. S.; Mirkin, C. A. *Angew. Chem., Int. Ed.* **2007**, *46*, 4093-4096. (f) Li, D.; Wieckowska, A.; Willner, I. *Angew. Chem. Int. Ed.* **2008**, *47*, 3927-3931. (g) Liu, S.-J.; Nie, H.-G.; Jiang, J.-H.; Shen, G.-L.; Yu, R.-Q. *Anal. Chem.* **2009**, *81*, 5724-5730. (h) Kong, R.-M.; Zhang, X.-B.; Zhang, L.-L.; Jin, X.-Y.; Huan, S.-Y.; Shen, G.-L.; Yu, R.-Q. *Chem. Comm.* **2009**, 5633-5635. (i) Guo, L.; Yin, N.; Chen, G. *The Journal of Physical Chemistry C* **2011**, *115*, 4837-4842. (k) Kiy, M. M.; Jacobi, Z. E.; Liu, J. *Chemistry – A European Journal* **2012**, *18*, 1202-1208. (l) Deng, L.; Zhou, Z. X.; Li, J.; Li, T.; Dong, S. J. *Chem. Comm.* **2011**, *47*, 11065-11067.

(31)   Pregibon, D. C.; Doyle, P. S. *Anal. Chem.* **2009**, *81*, 4873-4881.

(32)   Pregibon, D. C.; Toner, M.; Doyle, P. S. *Science* **2007**, *315*, 1393-1396.

(33)   Kawaguchi, H. *Prog. Polym. Sci.* **2000**, *25*, 1171-1210.

(34)   (a) Weizmann, Y.; Cheglakov, Z.; Willner, I. *J. Am. Chem. Soc.* **2008**, *130*, 17224-17225. (b) Pavlov, V.; Xiao, Y.; Gill, R.; Dishon, A.; Kotler, M.; Willner, I. *Anal. Chem.* **2004**, *76*, 2152-2156. (c) Zhang, X.-B.; Wang, Z.; Xing, H.; Xiang, Y.; Lu, Y. *Anal. Chem.* **2010**, *82*, 5005-5011. (d) Zhang, S. S.; Xia, J. P.; Li, X. M. *Anal. Chem.* **2008**, *80*, 8382-8388.

(35)   Huizenga, D. E.; Szostak, J. W. *Biochemistry* **1995**, *34*, 656-665.

(36)   (a) Jhaveri, S. D.; Kirby, R.; Conrad, R.; Maglott, E. J.; Bowser, M.; Kennedy, R. T.; Glick, G.;
         Ellington, A. D. *J. Am. Chem. Soc.* **2000**, *122*, 2469-2473. (b) Nutiu, R.; Li, Y. *J. Am. Chem. Soc.*
         2003, *125*, 4771-4778. (c) Tang, Z. W.; Mallikaratchy, P.; Yang, R. H.; Kim, Y. M.; Zhu, Z.;
         Wang, H.; Tan, W. H. *J. Am. Chem. Soc.* **2008**, *130*, 11268-11269. (d) Urata, H.; Nomura,
         K.; Wada, S.-i.; Akagi, M. *Biochem. Biophys. Res. Comm.* **2007**, *360*, 459-463.

(37)   (a) Xu, W. C.; Lu, Y. *Anal. Chem.* **2010**, *82*, 574-578. (b) Xiang, Y.; Tong, A. J.; Lu, Y. *J. Am.
         Chem. Soc.* **2009**, *131*, 15352-15357. (c) Zhou, Z.; Du, Y.; Dong, S. *Anal. Chem.* **2011**, *83*, 5122-
         5127. (d) Cheng, X. H.; Bing, T.; Liu, X. J.; Shangguan, D. H. *Anal. Chim. Acta* **2009**, *633*, 97-
         102. (e) Wang, Y. Y.; Liu, B. *Analyst* **2008**, *133*, 1593-1598. (f) Pei, R.; Stojanovic, M. N. *Anal.
         Bioanal. Chem.* **2008**, *390*, 1093-1099. (g) Zhou, Z.; Du, Y.; Dong, S. *Biosens.
         Bioelectron.* **2011**, *28*, 33-37.

(38)   Gudnason, H.; Dufva, M.; Bang, D. D.; Wolff, A. *Nucleic Acids Res.* **2007**, *35*, e127.